



Factors Affecting the performance of trickle dusters for preventing explosive dust accumulations in return airways

Michael J. Sapko^a, Marcia L. Harris^{a,*}, Inoka E. Perera^a, Isaac A. Zlochower^a, Eric S. Weiss^b

^a Pittsburgh Mining Research Division, National Institute for Occupational Safety and Health, United States

^b NIOSH, United States

ABSTRACT

Correctly applied rock dust can dilute, inert, and mitigate the explosive potential of float coal dust. Trickle dusters are one element of a comprehensive system to help prevent coal dust explosions in underground coal mines. Trickle dusters supply rock dust to inert fine float coal dust in areas where it is commonly deposited, such as the longwall tailgate returns, return airways, pillaring areas, and downwind of belt transfers. Dust deposition studies show that the effectiveness of trickle dusters depends on several key factors. Using multiple orifices, rock dust should be released near the mine roof in the direction of the airflow in order to spread the cloud cross the entry. The rock duster should have a mechanism to break up rock dust agglomerates as they leave the rock duster. The particle size distribution of the limestone rock dust and its airborne concentration should be proportional to the airborne size distribution and concentration of coal dust passing by the trickle duster. Specifically, rock dusts having a greater proportion of < 74 µm material are more effective at minimizing downwind zones of explosible mixtures than mostly larger particles. In our testing, rock dusts having more than 95% of < 74 µm sized particles were adequately dispersed by trickle dusters. Based on our results, the mass rate of rock dust discharge from the trickle duster should exceed the rate of float coal production by at least a factor of four in order to minimize accumulations of explosible dusts.

1. Background

Good rock dusting practices have been shown to prevent large float coal dust explosions. Simply stated, rock dust acts as a heat sink to remove the energy associated with a propagating coal dust explosion. Therefore, to effectively suppress a coal dust explosion, sufficient quantities of effective rock dust must be present at the mine entry so that the expanding explosion pressure wave entrains both coal dust and inerting rock dust [Cybulski 1975; Michelis et al., 1987; Michelis 1996; Reed and Michelis 1989; Lebecki 1991].

Rock dusting in mine entries dates back to the early 1900s. Since that time, coal mining practices have changed substantially and produce finer particles of coal dust, termed float coal dust. Since the Upper Big Branch Mine disaster, regulatory requirements and inspections to ensure that adequate quantities of rock dust are applied to the roof, ribs, and floor throughout the mine have become increasingly stringent in an effort to prevent coal dust explosions. In an effort to apply rock dust and keep pace with the generation of coal dust, many mines use trickle dusters, which disperse rock dust in working areas of a coal mine [Courtney et al., 1982].

Operators continue to face compliance issues and to search for rock dust application methods that comply with the standards with minimal operational impact. For example, the Mine Safety and Health Administration's (MSHA's) post-explosion dust sampling results

obtained as part of the Upper Big Branch Mine accident investigation indicated numerous locations at which non-compliant dust samples were found in the mine (MSHA, 2011). MSHA's analysis of the evidence showed that a limited amount of methane ignited and propagated into a massive coal dust explosion. The MSHA report concluded that continual rock dusting into the tailgate of longwalls, section returns, and other areas where float coal dust accumulates during mining is a proactive practice to inert float coal dust and to minimize the risk of an explosion [MSHA 2013]. MSHA's analyses of rock dust samples, sampling records, impact inspections, and other enforcement data indicate that combustible materials, coal dust, and float coal dust still accumulate at some underground coal mine operations. Some operations also did not have sufficient rock dust in all required areas. Violations of 30 CFR 75.403 (Maintenance of incombustible content of rock dust) rank fourth and third, with 1667 violations in 2015 and 2200 violations in 2014, respectively [MSHA 2016]. Compared to 2010 (981 violations), the number of violations cited in 2014 have doubled.

In coal mining, the dust deposition rate is important because it indicates how quickly explosible conditions can develop. Deposition measurements also provide a check on the adequacy of the rock dust used to minimize excessive accumulations of explosive coal dust. However, it is difficult to investigate the key factors of dust deposition in an active coal mine. The concentration of airborne dust varies continuously, and the airway geometries where the dust travels are

* Corresponding author.

E-mail address: ztv5@cdc.gov (M.L. Harris).

<https://doi.org/10.1016/j.jlp.2019.05.013>

Received 17 January 2019; Received in revised form 21 May 2019; Accepted 25 May 2019

Available online 28 May 2019

0950-4230/ © 2019 Elsevier Ltd. All rights reserved.

complicated. In the case of longwall tailgate entries, it is especially difficult to access and measure incombustible content.

The authors considered whether dust dispersion techniques and practices could be enhanced to improve the efficacy of rock dusting efforts and to increase compliance among mine operators. To this end, rock dust dispersion was studied to identify variables that may improve dust dispersion along the entire treated area. The effects of dust particle size, the size distribution of rock dust particles within a larger sample, and the effect of air velocity on rock dust dispersion in relation to coal dust deposition were examined. This paper summarizes the results of coal and rock dust deposition studies conducted within the Bruceton Experimental Mine (BEM) along with limited data collected from the tailgate of an operating longwall. Key operational factors for improving the effectiveness of trickle dusters as rock dust dispersal devices are also identified.

2. Dust settling

The terminal settling velocity of dust particles is derived by balancing drag, buoyancy, and gravitational forces on each particle. For diluted suspensions, Stokes' law predicts the settling velocity of spheres in air due to the viscous forces at the surface of the particle providing the majority of the retarding force. Stokes' law is given by the following equation:

$$\frac{g(\rho_p - \rho_a)D_p^2}{18\mu} = V_S \quad (1)$$

where V_S = terminal settling velocity (cm/s), g = gravitational constant (cm/s^2), ρ_p = density of the particle (g/cm^3), ρ_a = density of air (g/cm^3), D_p = particle diameter (μm), and μ = viscosity of the air ($\text{g/cm}^2\text{s}$).

At standard conditions, a simpler version of Equation (1) can be written for spheres:

$$V_S = 0.003\rho_p D_p^2 \quad (2)$$

The terminal settling velocity, V_S , increases rapidly as the square of particle diameter. The denser rock dust particles (2.7 g/cm^3) settle about two times faster than the less dense coal dust particles (1.35 g/cm^3) of the same diameter. To settle at the same location downwind, the average diameter of a rock dust particle must be 0.7 times that of an average coal dust particle.

When particles are dispersed near the roof of height H (m) in a mine tunnel with an average airflow of V_o (cm/s), the distance, X (m), downwind where a particle settles on the floor can be estimated by:

$$X = H \frac{V_o}{V_S} \quad (3)$$

The location, X_{CD} , where a coal particle settles on the mine floor is given by the product of the ratio of the densities of the rock dust and coal dust particles (ρ_{RD}/ρ_{CD}) and the settling distance of a rock dust particle of similar diameter, X_{RD} .

$$X_{CD} = X_{RD} \left(\frac{\rho_{RD}}{\rho_{CD}} \right) = 2X_{RD} \quad (4)$$

By substituting V_S from Equation (2) into Equation (3) and solving for D_p , the mean particle diameter decreases as $\frac{1}{\sqrt{X}}$ with distance, X , downwind:

$$D_p = \sqrt{\frac{V_o H}{0.003\rho_p X}} \quad (5)$$

There are many dust propagation and deposition models that were developed specifically for the underground mining industry and mostly driven by the regulatory environment (NIOSH, 2005). A simplified Gaussian model is being developed and validated with this

experimental deposition data from the BEM. The simple model and its methods of application will be presented in a follow-up publication. The authors anticipate that the model can help mine operators make more effective use of their trickle dusters by providing a better downwind incombustible balance between the mining-generated coal dust and the distributed rock dust. Input parameters include the coal and rock dust particle distributions at the trickle duster, average ventilation rate, entry geometries, coal dust generation rates, and the rate of rock dust discharge from the trickle duster.

2.1. Experimental procedure

The dust deposition study described in this paper was mostly carried out in the BEM under controlled conditions. Limited deposition data was also collected from one tailgate entry at a participating coal mine.

2.2. BEM test conditions

Pittsburgh Mining Research Division (PMRD) researchers conducted studies within the BEM to examine the effect of variations in rock dust particle size and their ability to provide an inerting balance between the aerodynamically deposited float coal dust and rock dust applied using pneumatic rock dusters.

The main entry of the BEM was used to perform controlled dust deposition experiments. The single entry is nominally 2.74 m wide by 2.2 m high and 396 m long. A variable-speed fan provided the ventilating air for the dust dispersion studies.

Fifteen dust deposition experiments were conducted in the BEM. Seven experiments were conducted with three rock dusts (RD 1, RD 2, and RD 3) and at two airflows—an average high airflow of about 1.5 m/s and an average low of about 0.6 m/s. Eight experiments were conducted with either 10% or 20% of coal dust mixed with the previously mentioned three rock dusts and an additional rock dust (RD 4). The mixtures were also conducted at high and low ventilation flow rates (Table 1). RD 1 and RD 2 are commercially available and used in coal mines. RD 3 is an anti-caking rock dust developed under a NIOSH BAA agreement (Imerys, 2014), and RD 4 consisted of a commercial rock dust having only ~7% of < 10 μm particles. The coal dust used in these tests is from the same coal seam and has similar particle size distributions as those used in large-scale inerting studies conducted at the Lake Lynn Experimental Mine (LLEM) (NIOSH, 2010).

The differential volume percent and cumulative volume percent size distributions of the four commercial rock dusts and the Pittsburgh seam pulverized coal dust used in these experiments are shown in Fig. 1. The particle size distributions of the dispersed coal dust, rock dust, and the deposited mixtures were determined using a Beckman-Coulter LS 13,320 Laser Diffraction Particle Size Analyzer equipped with a Tornado Dry Powder System (B–C). The refractive index (RI) used for all rock dust samples is $1.68 + 0.0i$ (i.e., no absorptive component) as it is the value listed in the B–C manual for calcium carbonate. The RI used for all coal dust samples has a significant imaginary component (it is strongly absorbing) and is $1.80 + 0.3i$. The particles were treated as equivalent spherical light scatterers (Mie scattering). Note that all rock dusts, except RD 4, exhibit bimodal distributions.

To minimize the potential formation of dispersed clouds of explosible mixtures in the BEM's single entry during testing, coal dust and rock dust mixtures of 80% and 90% by mass rock dust were thoroughly mixed by tumbling in 32-gal drums before loading the rock duster for test dispersion. A total of 183 kg of each mixture was dispersed for each test except for tests 14 and 15, where 91 kg were dispersed.

The mid-stream average air velocity for each experiment was measured at all sampling stations using a Davis vane anemometer, and the average volumetric airflow was calculated based upon the entry dimensions. The dust was distributed using an A.L. Lee EL5-200 battery-powered rock duster with the air-dust discharge through a 5-cm diameter nozzle attached to the roof (Fig. 2).

Table 1

Correlation of mass deposition and mean particle diameter 18.3–152.4 m downwind of the rock duster.

Test #	Dust	Air flow, cm/s	Mass Deposition			Mean Diameter		
			$g/m^2 = cX^k$			$D_m = aX^b$		
			c	k	R ²	a	b	R ²
1	80% RD 1/20% CD	58	100,000	−1.88	0.96	96	−0.53	0.98
2	RD 1	59	36,000	−1.57	0.96	53	−0.44	0.97
3	80% RD 2/20% CD	60	99,000	−1.87	0.99	82	−0.44	0.99
4	RD 2	59	64,000	−1.86	0.98	73	−0.44	0.99
5	80% RD 1/20% CD	163	198,000	−1.90	0.99	182	−0.56	0.98
6	RD 1	139	69,000	−1.78	0.99	103	−0.51	0.96
7	80% RD 2/20% CD	169	493,000	−2.04	0.99	136	−0.46	0.97
8	RD 2	147	579,000	−2.10	0.99	98	−0.41	0.99
9	RD 3	70	222,000	−2.03	0.99	139	−0.53	0.99
10	RD 3	40	71,000	−1.81	0.99	109	−0.57	0.99
11	RD 2	46	45,000	−1.93	0.99	88	−0.47	0.99
12	90% RD 3/10% CD	46	95,000	−1.91	0.99	127	−0.57	0.99
13	90% RD 3/10% CD	100	375,000	−2.09	0.99	206	−0.58	0.99
14	90% RD 4/10% CD	64	477,000	−2.42	0.98	57	−0.27	0.99
15	90% RD 4/10% CD	124	170,000	−2.13	0.99	48	−0.22	0.98

X from 18 to 152 m downwind.

Dust was dispersed in two 91-kg) batches, each batch requiring about 20–40 min to disperse. The rock dust discharge rate was not constant. It varied with the size distribution of the rock dust, the depth of dust in the hopper, and dust hang-up on the walls of the hopper. Settled dust was collected on metal dust collection trays measuring 23 cm wide by 33 cm long, and approximately $\sim 800 \text{ cm}^2$ in area. These were placed on the experimental mine concrete floor, rib shelves, and center post shelves downwind of the rock duster.

Settled dust was also collected on 1.2-m x 1.8-m-1.9-cm thick plywood that was covered with waxed butcher block paper. Samples collected from the tailgate entry of a participating mine were collected by brushing off predetermined marked sections of the ground support cribs.

2.3. Longwall mine test conditions

The experimental procedure used at an active longwall mine was different from that used in the BEM. The longwall operation used pressurized air to entrain and push rock dust through a flexible duct along the ground support shields starting at the headgate and ending at the tailgate, which is a distance of $\sim 305 \text{ m}$ in length. At the tailgate, rock dust was injected through a 5.1-cm diameter pipe positioned at mid-entry height near the last shield. Coal dust produced by the shearer was carried along the ventilation path towards the injection pipe. The movement of ground support shields also produced dust that remained



Fig. 2. Air-dust discharge through a 2-in (5.1-cm) diameter tube attached to the roof 7.25 ft (2.2 m) above the floor.

airborne, mixing with the rock dust near the last shield before being carried with the ventilating air into the return airway. Before the longwall startup at the beginning of the shift, ground support cribs adjacent to the coal pillar were wiped clean, and metal trays were

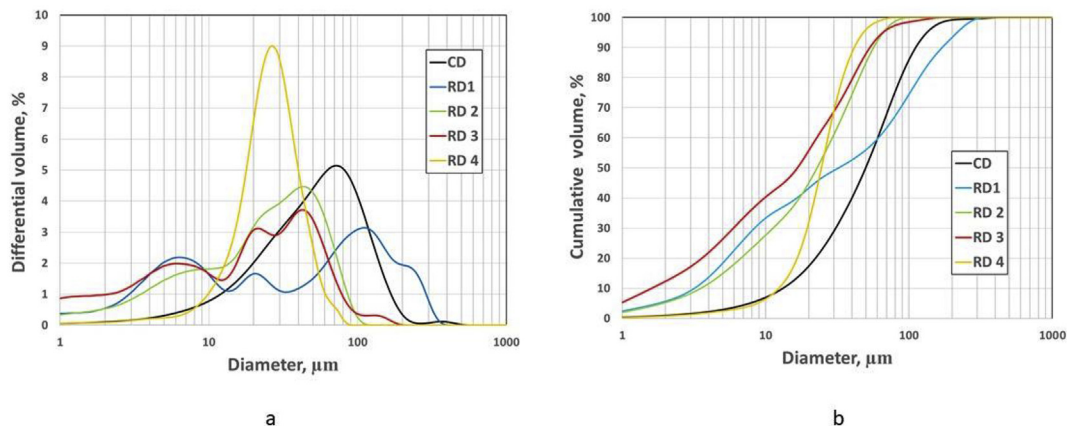


Fig. 1. Complete differential volume % with (a) cumulative volume % and (b) size distributions of the coal dust and rock dusts used in BEM deposition experiments.

placed mid-entry on the floor and spaced 6 m apart starting at the longwall panel. After three days, when the longwall shut down for routine system checks and repairs, dust samples were collected. Using a soft bristled brush, the support crib dust samples were gathered at distances 3, 12, and 24 m from the tailgate. Other dust samples were collected from the remaining 8 metal trays that were not lost to the gob as the coal face advanced.

2.4. Post-test analysis

After the dust cleared the entry, the dust samples were collected from each tray or crib surface, sealed in an air-tight plastic bag, and brought to the surface for analysis. After drying, the samples were weighed using a Mettler balance, to the nearest 0.01 g, and then underwent a particle size analysis using the B–C. The rock dust content of the deposited coal dust and rock dust mixtures was determined using the low-temperature ashing (LTA) method which burns off the coal component at 515 °C (Montgomery, 2005; NIOSH, 2010).

3. Results

The focus of this research was to demonstrate how coal dust and rock dust particles settle out of the ventilating air and to identify the factors that impact the formation of explosible coal and rock dust zones downwind of trickle dusters.

Studies were designed to experimentally determine and numerically model the time and distance for coal and rock dust particles to deposit under various airflow conditions and initial particle size distributions. Researchers also wanted to determine the potential impact of any aerodynamic size classification that may occur between the coal and rock dust particles and its potential impact on inerting explosible accumulations of float coal dust.

3.1. Rock dust

Shown in Fig. 3, the experimental results from Test 9 serve as a representative example of the measured floor mass deposition (g/m^2) and mean particle diameter D_m variations with distance downwind of the discharge point. The results indicate that the mass deposited downwind follows a logarithmic decay from $x = 18.3$ –152 m proportional to $\sim 1/x^2$, while the decay mean diameter is proportional to $\sim 1/\sqrt{x}$. The decay of mass deposition and mean diameter is particularly consistent for Tests 1–13 as listed in Table 1, which shows the respective correlations for the 15 experiments conducted in the BEM.

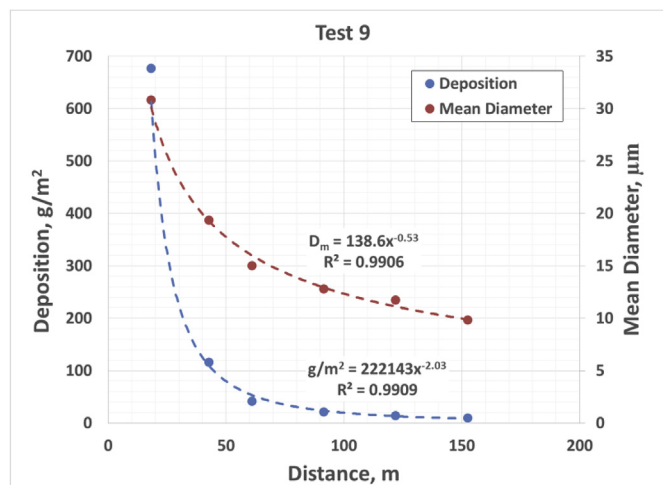


Fig. 3. An example of mass deposition and mean particle size measurements of samples collected from the mine floor downwind of the rock duster during Test 9.

The differential and cumulative size distributions for RD 1 and for floor samples collected afterwards at various distances downwind are shown in Fig. 4 for Test 2. This data shows that 38% of particles by mass $> 74 \mu\text{m}$ in size dropped out of the air within 18.3 m of the rock duster. This left only about 62% of the released mass of rock dust to inert coal dust at greater distances.

Dispersing RD 2 under the same ventilation conditions (Test 4) yielded the data shown in Fig. 5a and b. The cumulative size distributions of Test 4 with RD 2 (Figure 5b) are similar to the original RD 2 except that only 4% of particles $> 74 \mu\text{m}$ settle out within 18.3 m. Consequently, 96% of the particle mass $< 74 \mu\text{m}$ is able to travel downwind to inert coal dust.

3.2. Mixtures of coal and rock dust

Variations in rock dust particle size distributions and mass percentages $< 74 \mu\text{m}$, such as those shown in Fig. 1, were expected to produce different inerting effects downwind of the trickle duster. To help illustrate the extent of inerting differences, eight experiments with coal and rock dust mixtures (Table 1) were conducted in the BEM. The 80/20 (RD 1/CD) mixture and the 80/20 (RD 2/CD) mixture were dispersed in separate experiments (Tests 1, 3, 5, and 7) at the two different air velocities listed in Table 1. The deposited samples were collected and analyzed.

Shown in Figs. 6 and 7 are the particle size distributions of the coal and rock dust mixtures and of the samples collected from the floor at various distances from the rock duster for Test 5 and Test 7, respectively. A mixture of 80% RD1 and 20% CD was dispersed in Test 5. Approximately 33% of RD 1 is $< 74 \mu\text{m}$ in size. As the mixture is discharged from the rock duster, the larger coal and rock dust particles in the range of $74 \mu\text{m}$ – $250 \mu\text{m}$ settle on the floor within 5 m–9 m from the source. Due to the varying particle sizes and densities, the rock dust and coal dust particles settle out of the airstream at differing rates and times. The resulting effects on the total incombustible content are seen in Fig. 8. The total incombustible content increases to 97% within 9 m of release. This is substantially higher than the 80% rock dust concentration originally dispersed. Between 9 and 15 m, however, the concentration of rock dust rapidly decreases to 70%, which is less than the 80% incombustible content required in 30 CFR 75.403. At 60 m, the percentage of rock dust returns to the non-explosive range and remains $\geq 80\%$ for the remainder of the samples.

The rock dust used in Test 7, RD 2, contains only 2% $> 74 \mu\text{m}$ particles. The 84.5% incombustible content of the floor samples at 9 m is similar to the concentration in the initial sample (80%). The concentration of rock dust drops to 76% at approximately 12 m but then rapidly returns to 80% at 18 m. The concentration continues to increase, building to about 85% at 40 m, and remains $> 85\%$ for the remainder of the samples.

These results indicate that a rock dust containing $\sim 33\%$ of $> 74 \mu\text{m}$ particles left an area $> 50 \text{ m}$ inadequately rock dusted. This could have a significant impact on the size and variation of explosive zones. Rock dusts with smaller percentages of particles $> 74 \mu\text{m}$ produced improved rock dust coverage downwind of application.

Air velocity also has an effect on the location and extent of inert and explosive zones downwind of the rock duster (Fig. 9). Comparing downwind inerting results between Test 3 using RD 2 at 0.6 m/s with Test 7 using RD 2 at 1.63 m/s, the zones with $< 80\%$ rock dust increase from essentially none at the low airflow to 10 m (7 m–17 m from the rock duster) with the higher airflow. The explosive zone when using RD 1 is even greater, extending from $\sim 25 \text{ m}$ to 50 m in length with increasing airflows.

Additional Tests 12, 13, 14, and 15 consisted of mixtures created with 90% rock dust uniformly mixed with 10% CD. These tests were conducted to explore the extent to which the combined effect of increasing air velocity and the relative amount of rock dust particles $< 10 \mu\text{m}$ would have on the dust mixtures' abilities to inert

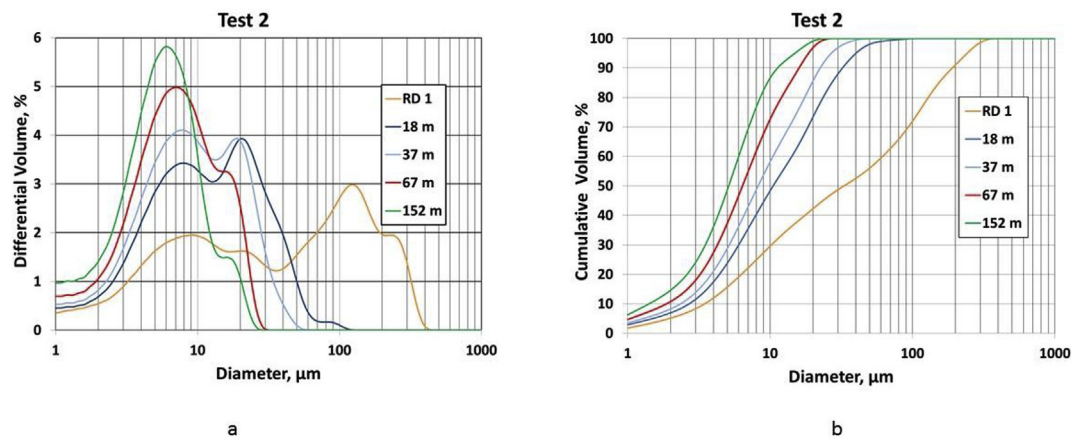


Fig. 4. The measured differential volume % with (a) cumulative volume % and (b) particle size distributions of the original dust dispersed (RD 1) and of the floor samples collected at various distances downwind for Test 2.

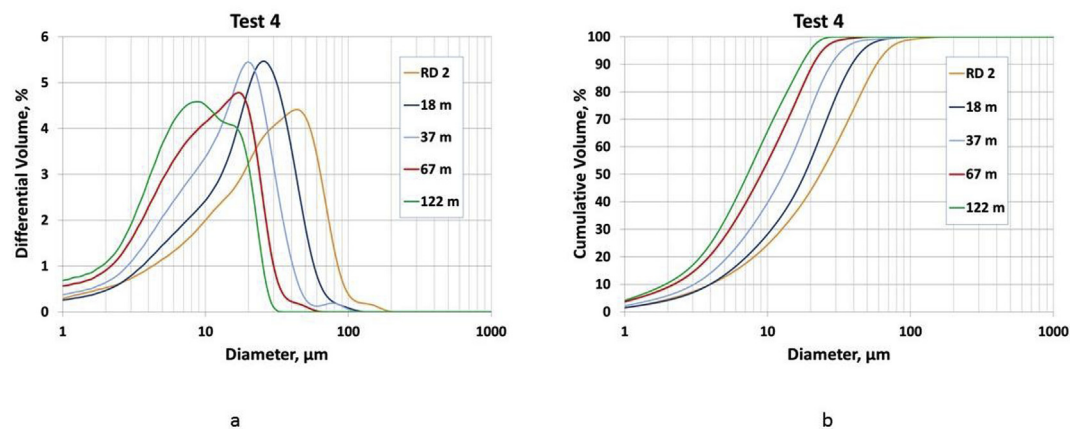


Fig. 5. The measured differential volume % with (a) cumulative volume % and (b) particle size distributions of the original dust dispersed (RD 2) and of the floor samples collected at various distances downwind for Test 4.

over longer distances. Two rock dusts, RD 3 ($\sim 42\% < 10 \mu\text{m}$) and RD 4 ($\sim 6\% < 10 \mu\text{m}$), were used in these experiments (Fig. 10). The rock dust percentages in Tests 12 and 13 continued to increase with distance and decrease with increasing velocity over the same space. These trends are similar to those observed for Tests 1 and 5 where the rock dust contained $\sim 32\% < 10 \mu\text{m}$. Since RD 4 contains only $\sim 6\% < 10 \mu\text{m}$ particles, the rock dust percentages measured in Tests 14 and 15 continued to decrease with increasing distance and ventilation velocity.

3.3. Longwall tailgate dust samples

The PMRD researchers, as part of another study examining mine dust sampling methods, had the opportunity to collect dust samples from ground supports and trays placed in a tailgate entry of a longwall panel. Although these experimental data are limited, the results are presented here for completeness.

At the crib locations $\sim 3 \text{ m}$, $\sim 12 \text{ m}$, and $\sim 24 \text{ m}$ inby the tailgate

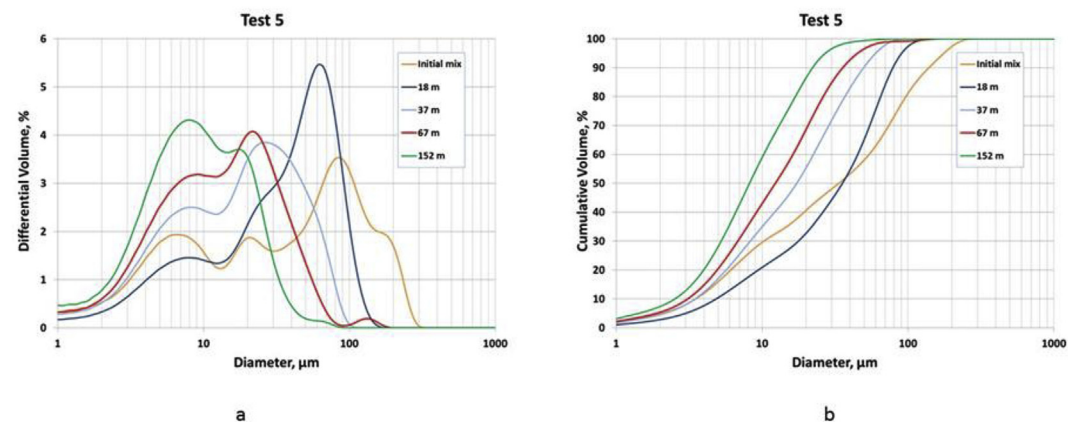


Fig. 6. The measured differential volume % with (a) cumulative volume % and (b) particle size distributions of the original rock dust/coal dust mixture dispersed (initial mix) and of the floor samples collected at various distances downwind for Test 5.

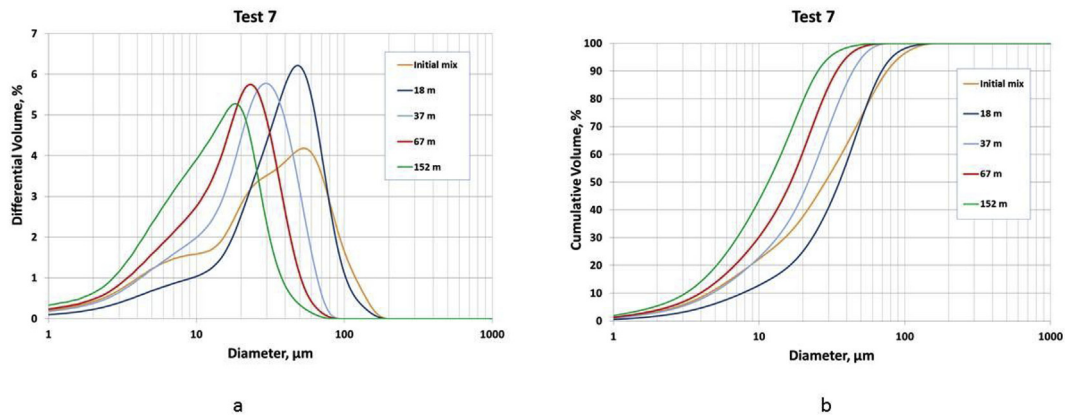


Fig. 7. The measured differential volume % with (a) cumulative volume % and (b) particle size distributions of the original rock dust/coal dust mixture dispersed (initial mix) and of the floor samples collected at various distances downwind for Test 7.

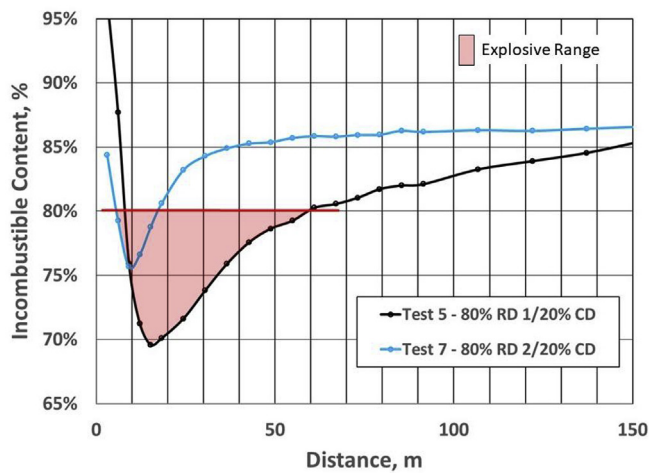


Fig. 8. Comparison of the explosive zone lengths formed in Test 5 using RD 1 and Test 7 using RD 2. The red shaded area below 80% incombustible content indicates the explosive range. (For interpretation of the references to colour in this figure legend, the reader is referred to the Web version of this article.)

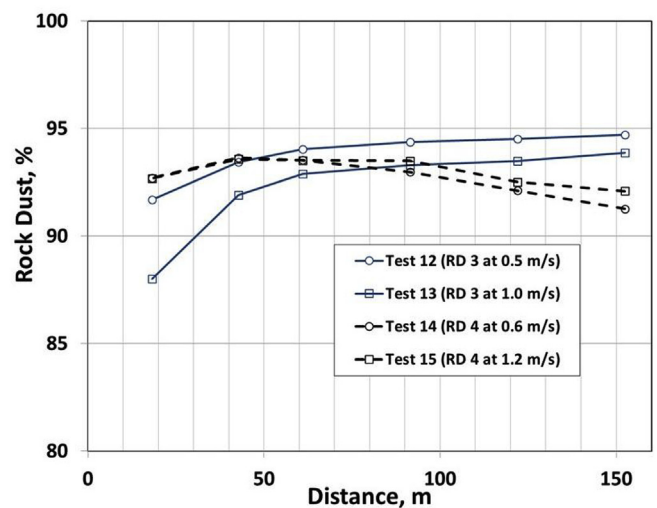


Fig. 10. Comparison of the explosive zone lengths formed in Tests 12, 13, 14, and 15 for mixtures of 90% RD 3 and RD 4 and 10% CD conducted at two air velocities.

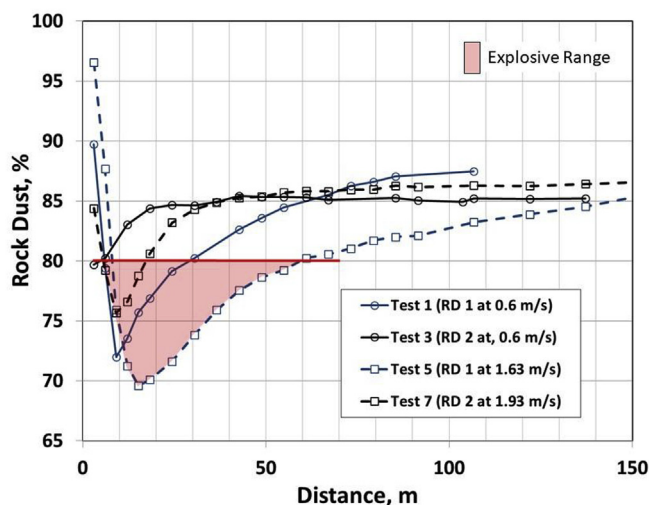


Fig. 9. Comparison of the explosive zone lengths formed in Tests 1, 3, 5, and 7 for mixtures of 80% RD 1 and RD 2 and 20% CD conducted at two air velocities. The red shaded area below 80% incombustible content indicates the explosive range. (For interpretation of the references to colour in this figure legend, the reader is referred to the Web version of this article.)

corner, the measured mean diameters were 36, 33, and $7\text{ }\mu\text{m}$, respectively. Fig. 11 shows the changes in particle size distribution. These results cannot be directly compared to the BEM deposition studies since the size distribution of the combined coal dust and rock dust leaving the tailgate changes with the advancement of the face and the movement of the shearer across the $\sim 305\text{-m}$ longwall panel. When the longwall dust samples were collected, the air split at the tailgate entry with more air flowing outby along the coal block and less air flowing towards the gob. Within 3 m of the face, 90% of the coal and rock dust particles collected from cribs were less than $74\text{ }\mu\text{m}$. At 24 m, 98% of the collected coal and rock dust particles were less than $30\text{ }\mu\text{m}$. Incombustible results indicate that the total incombustible content increased from 72% at 3 m from the face to 82% at 24 m.

4. Conclusions

These results suggest that when using trickle dusters in return airways and belt entries to minimize the zones of explosive coal dust and rock dust mixtures, a finer-sized dispersible rock dust provides a better inerting balance for the reference coal dust over longer distances downwind. Particles $> 74\text{ }\mu\text{m}$ in size fall out of suspension very close to the release point.

The effective inerting balance of deposited coal and rock dust mixtures depends on the size distribution of the coal dust passing by the

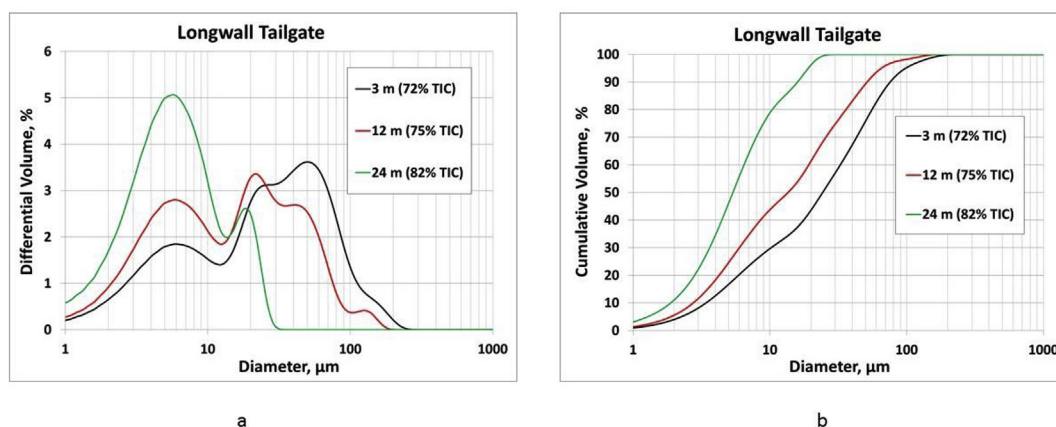


Fig. 11. The measured differential volume % with (a) cumulative volume % and (b) particle size distributions of mine dust samples collected from the return airway of a longwall. The incombustible content is also indicated in the legend for each distance from the longwall.

rock duster and the size distribution of the rock dust being dispersed into the airflow. The finer rock dust is better able to follow and settle with the fine coal dust produced by modern mining activities. The total dispersed mass of rock dust dispersed by the duster should be at least four times the mass generation rate of the coal dust to meet the 80% total incombustible content requirement.

Disclaimer

Mention of any company or product does not constitute endorsement by the National Institute for Occupational Safety and Health. The findings and conclusions in this paper are those of the authors and do not necessarily represent the views of NIOSH.

Acknowledgements

The authors acknowledge NIOSH PMRD Physical Science Technicians, Linda Chasko and James Addis, for their exceptional contributions in preparing and conducting the large-scale deposition experiments and the post-test analyses.

References

- Courtney, W.G., Kost, J., Colinet, J.F., 1982. Dust Deposition in Coal Mine Airways. U.S. Department of the Interior, Bureau of Mines, Pittsburgh, PA Technical Progress Report (TPR) 116. NTIS No. PB 82-194853.
- CFR, Code of Federal Regulations. Washington, DC: U.S. Government Printing Office, Office of the Federal Register.
- Cybulski, W.G., 1975. Coal Dust Explosions and Their Suppression. National Center for Scientific, Technical and Economic Information. NTIS No. TT 73-54001, Warsaw, Poland Translated from Polish.
- Imerys, 2014. Development of an Anti-caking Rock Dust. NIOSH Broad Agency Announcement (BAA) 2012-N-14257, Contract # 200-2012-52496), April 2014.
- Lebecki, K., 1991. Gas dynamics of coal dust explosion—theory and experiment. In: Proceedings of the 24th International Conference of Safety in Mines Research Institutes (Donetsk, USSR, September 23–28), vol. 1. pp. 357–373.
- Michelis, J., 1996. Large scale experiments with coal dust explosions in connection with road-T-junctions. In: The Seventh International Colloquium on Dust Explosions; Part of the International Symposium on Hazards, Prevention and Mitigation of Industrial Explosions (Bergen, Norway, June 23–26, 1996). Christian Michelsen Research, pp. 8.50–8.59.
- Michelis, J., Margenbarg, B., Müller, G., Kleine, W., 1987. Investigations into the buildup and development conditions of coal dust explosions in a 700-m underground gallery. In: Cashdollar, K.L., Hertzberg, M. (Eds.), Industrial Dust Explosions. American Society for Testing and Materials (ASTM), Special Technical Publication (STP) 958, West Conshohocken, PA, pp. 124–137.
- Montgomery, T., 2005. Personal Communications on Incombustible Analysis Procedures. MSHA, 2011. Fatal Underground Mine Explosion, April 5, 2010. Performance Coal Company Upper Big Branch Mine—South, Massey Energy Company Mine ID: 46-08436. Mine Safety and Health Administration December 6, 2011.
- MSHA, 2013. Program for Regular Cleanup and Removal of Accumulations of Coal and Float Coal Dust, Loose Coal, and Other Combustibles. Program Policy Letter No. P13-V-11, December 18, 2013. <http://www.msha.gov/regs/compliance/ppls/2013/PPL13-V-11.asp> December 6, 2011.
- MSHA, 2016. Most Frequently Cited Standards for 2015 Underground – Coal. <http://arlweb.msha.gov/stats/top20viols/top20viols.asp>, Accessed date: 11 January 2016.
- NIOSH, 2005. Significant Dust Dispersion Models for Mining Operations. By Reed WR: U.S. Department of Health and Human Services, Centers for Disease Control and Prevention, National Institute for Occupational Safety and Health. DHHS (NIOSH) Publication No. 2005-138.
- NIOSH, 2010. Recommendations for a new rock dusting standard to prevent coal dust explosions in intake airways. In: Cashdollar, K.L., Sapko, M.J., Weiss, E.S., Harris, M.L., Man, C.K., Harteis, S.P., Green, G.M. (Eds.), U.S. Department of Health and Human Services, Centers for Disease Control and Prevention, National Institute for Occupational Safety and Health. DHHS (NIOSH) Publication No. 2010-151.
- Reed, D., Michelis, J., 1989. Comparative investigation into explosibility of brown coal and bituminous coal dust in surface and underground test installations. In: Proceedings of the 23rd International Conference of Safety in Mines Research Institutes (Washington, DC, September 11–15, 1989). U.S. Department of the Interior, Bureau of Mines, Pittsburgh, PA, pp. 941–964.